Evolution of the vortex state in the BCS–BEC crossover of a quasi two-dimensional superfluid Fermi gas*

Xuebing Luo(罗学兵), Kezhao Zhou(周可召)†, and Zhidong Zhang(张志东)

Shenyang National Laboratory for Materials Science, Institute of Metal Research, Chinese Academy of Sciences, Shenyang 110016, *China*

(Received 30 March 2016; revised manuscript received 28 June 2016; published online 28 September 2016)

We use the path-integral formalism to investigate the vortex properties of a quasi-two dimensional (2D) Fermi superfluid system trapped in an optical lattice potential. Within the framework of mean-field theory, the cooper pair density, the atom number density, and the vortex core size are calculated from weakly interacting BCS regime to strongly coupled while weakly interacting BEC regime. Numerical results show that the atoms gradually penetrate into the vortex core as the system evolves from BEC to BCS regime. Meanwhile, the presence of the optical lattice allows us to analyze the vortex properties in the crossover from three-dimensional (3D) to 2D case. Furthermore, using a simple re-normalization procedure, we find that the two-body bound state exists only when the interaction is stronger than a critical one denoted by G_c which is obtained as a function of the lattice potential's parameter. Finally, we investigate the vortex core size and find that it grows with increasing interaction strength. In particular, by analyzing the behavior of the vortex core size in both BCS and BEC regimes, we find that the vortex core size behaves quite differently for positive and negative chemical potentials.

Keywords: ultra-cold quantum gases, superconductivity/superfluidity, vortex, BCS–BEC crossover

PACS: 03.75.Ss, 03.75.Lm, 37.10.Jk **DOI:** 10.1088/1674-1056/25/11/110306

1. Introduction

Since the first observation of Bose–Einstein condensation and Fermi superfluid phenomenon in ultracold atoms system,[1–9] tremendous attention in condensed matter community has been paid to this system both theoretically and experimentally[10–17] because of its high controllability. In particular, using the Feshbach resonance technique,[18,19] one can tune the two-body interaction at will. This unique feature of controlling interaction continuously provides an ideal platform to investigate the crossover from the weakly interacting BCS[20] regime with loosely bound cooper pairs to the strongly attractive region where tightly bound molecules form a Bose–Einstein condensate (BEC)[21,22] (BCS–BEC crossover). Furthermore, by adding a trapping potential in selective directions, the system can evolve from higher dimension to lower one in a continuous way. Among many interesting phenomena related with this cold atoms system, the vortex state is one of the most important, which receives much attention in both cold atoms[23–25] and condensed matter communities.[26–32] The vortex state in the BCS–BEC crossover has been investigated in great detail[33–36] by numerically solving the Bogoliubov–de Gennes (BdG) equation[37] and mean-field equations.[38–40] However, the vortex state and its properties in the dimensional crossover scenario have largely been untouched, which is the main focus of this paper.

We investigate the evolution of the vortex structure in both the BCS–BEC and the three dimensions (3D) to two dimensions (2D) crossover problems in a two-component Fermi gas trapped in an optical lattice potential at zero temperature. The main results are composed of two parts. First, the atom number density and the pair density (gap profile) are calculated for different interaction strengths and lattice potential parameters. We identify the BCS and BEC regimes by the existence of the bound state and the boundary can be given by a critical interaction strength which is a function of the lattice potential parameter. In the BCS regime, the Fermi atoms can penetrate into the vortex core, which is characterized by the nonzero atom density inside the vortex core where the pair density is zero. But in the BEC regime, the Fermi atoms cannot penetrate into the vortex core. The second part deals with the vortex core size as a function of the interaction strength and the lattice potential parameters. In the BCS regime where the chemical potential is positive in the bulk, the vortex core size is proportional to the square-root of the chemical potential determined by the atom number density equation. However, in the BEC limit with a negative bulk chemical potential, the vortex core size is determined by the gap equation.

The outline of the rest of this paper is as follows. In Section 2, we introduce the grand canonical partition function for a two-component Fermi gas in the presence of an optical lattice potential. Using the Hubbard–Stratonovic transformation, we rewrite the partition function as functional integral over pairing fields. Choosing the saddle point solution suitable for the description of the vortex state, we obtain the ground state energy and consequently the atom number and gap equations. Section 3 presents a detailed numerical evaluation of the atom number and gap equation profiles of the vortex state in the BCS–BEC crossover. We also discuss the dimensional effects

*Project supported by the National Natural Science Foundation of China (Grant Nos. 51331006, 51590883, and 11204321) and the Project of Chinese Academy of Sciences (Grant No. KJZD-EW-M05-3).

†Corresponding author. E-mail: kezhaozhou@gmail.com

© 2016 Chinese Physical Society and IOP Publishing Ltd

introduced by the optical lattice potential on the vortex structure. In Section 4, the vortex core size is calculated in the BCS–BEC crossover and the effect of the lattice potential is discussed. Finally, we summarize our results in Section 5.

2. Model Hamiltonian and mean field approximation

We consider a 3D two-component Fermi gas with an attractive two body interaction confined in an optical lattice potential. In the path integral formalism, the system can be described by the following grand-partition function at finite temperature T (we use the convention $\hbar = k_{\mathrm{B}} = 1$ throughout this paper):

$$\mathcal{Z} = \int \mathcal{D}[\bar{\psi}_\sigma, \psi_\sigma] \exp\{-S[\bar{\psi}_\sigma, \psi_\sigma]\}, \tag{1}$$

where $\bar{\psi}_\sigma$ and ψ_σ are the Grassmann fields [41] as functions of space and imaginary time τ. The action functional

$$\begin{aligned} S[\bar{\psi}_\sigma, \psi_\sigma] = & \int_0^\beta \mathrm{d}\tau \int \mathrm{d}\boldsymbol{r} \Big[\sum_\sigma \bar{\psi}_\sigma \left(\partial_\tau + \hat{\xi}_{\boldsymbol{p}} + V_{\mathrm{opt}}(\boldsymbol{r}) \right) \psi_\sigma \\ & - g \psi_\uparrow^\dagger \psi_\downarrow^\dagger \psi_\downarrow \psi_\uparrow \Big], \end{aligned} \tag{2}$$

where $\beta = 1/T$, the kinetic energy operator $\hat{\xi}_{\boldsymbol{p}} = \hat{\boldsymbol{p}}^2/(2m) - \mu$ with momentum operator $\hat{\boldsymbol{p}} = -\mathrm{i}\nabla$, m being the mass of the Fermionic atom, μ the chemical potential, and $g > 0$ denotes the s-wave interaction parameter. $V_{\mathrm{opt}}(\boldsymbol{r}) = sE_{\mathrm{R}} \sin^2(q_{\mathrm{B}} z)$ is the optical lattice potential along the z direction, where s denotes the intensity of the laser beam and $E_{\mathrm{R}} = \hbar^2 q_{\mathrm{B}}^2/2m$ is the recoil energy with q_{B} being the Bragg momentum. The lattice period is fixed by $q_{\mathrm{B}} = \pi/d$ with d being the lattice spacing. The atoms are free in the x–y plane. In order to investigate the pairing phenomena, we can re-write the partition function by introducing a Bosonic pairing field Δ using the Hubbard–Stratonovic transformation[41]

$$\mathcal{Z} = \int \mathcal{D}[\bar{\Phi}, \Phi; \bar{\Delta}, \Delta] \exp\{-S_{\mathrm{c}}[\bar{\Phi}, \Phi; \bar{\Delta}, \Delta]\}, \tag{3}$$

where

$$S_{\mathrm{c}}[\bar{\Phi}, \Phi; \bar{\Delta}, \Delta] = \int_0^\beta \mathrm{d}\tau \int \mathrm{d}\boldsymbol{r} \bar{\Phi} G^{-1} \Phi + \int_0^\beta \mathrm{d}\tau \int \mathrm{d}\boldsymbol{r} \frac{1}{g} \bar{\Delta}\Delta, \tag{4}$$

with $\Phi \equiv [\psi_\uparrow, \bar{\psi}_\downarrow]^{\mathrm{T}}$ and $\boldsymbol{G}^{-1}$ being the inverse Green's function

$$\boldsymbol{G}^{-1} = \begin{bmatrix} \partial_\tau + \hat{\xi}_{\boldsymbol{p}} + V_{\mathrm{opt}}(\boldsymbol{r}) & -\Delta \\ -\bar{\Delta} & \partial_\tau - \hat{\xi}_{\boldsymbol{p}} + V_{\mathrm{opt}}(\boldsymbol{r}) \end{bmatrix}. \tag{5}$$

Integrating out the Grassmann fields, we obtain

$$\mathcal{Z} = \int \mathcal{D}[\Delta, \bar{\Delta}] \exp\{-S_{\mathrm{eff}}[\Delta, \bar{\Delta}]\}, \tag{6}$$

with

$$S_{\mathrm{eff}} = \int_0^\beta \mathrm{d}\tau \int \mathrm{d}\boldsymbol{r} \frac{|\Delta(\boldsymbol{r}, \tau)|^2}{g} - \mathrm{Tr}\ln\left[\boldsymbol{G}^{-1}\right]. \tag{7}$$

By transforming the Grassmann integral into a Bosonic one, this path integral formalism provides a convenient framework to study the pairing phenomena. By properly choosing the saddle point solution, one can reduce the current formalism into the familiar mean-field BCS theory for different pairing symmetries. For example, in the absence of vortex state, we have the trivial saddle point solution $\Delta(\boldsymbol{r}, \tau) = \Delta_0$ and the thermodynamic potential becomes

$$\begin{aligned} \Omega_0 = \frac{S_{\mathrm{eff}}}{\beta} = & V \frac{\Delta_0^2}{g} + \sum_{\boldsymbol{k},n} (\xi_{\boldsymbol{k},n} - E_{\boldsymbol{p},n}) \\ & - \frac{2}{\beta} \sum_{\boldsymbol{k},n} \ln\left(1 + \mathrm{e}^{-\beta E_{\boldsymbol{k},n}}\right), \end{aligned} \tag{8}$$

where V is the volume of the system, $\xi_{\boldsymbol{k},n}$ denotes the band energy in the presence of the optical lattice potential, and the excitation spectrum reads $E_{\boldsymbol{p},n} = \sqrt{\xi_{\boldsymbol{k},n}^2 + \Delta_0^2}$. As one can see, even within the mean-field theory, one still has to calculate the noninteracting band energy spectrum to solve the mean-field equations. In this paper, we only consider the case where s is relatively large such that the inter band gap is far greater than the chemical potential μ and the tight-binding approximation applies. Within this approximation, the system can be well described by replacing the spectrum along the z direction by a Hubbard-type spectrum[42] $\varepsilon_{\boldsymbol{k}} = (1/2m)(k_x^2 + k_y^2) + 2t[1 - \cos(k_z d)]$, with t being the tunneling parameter which can be obtained in the tight binding limit as[11] $t = (4E_{\mathrm{R}}/\pi)(s/E_{\mathrm{R}})^{3/4} \exp\left(-2\sqrt{s/E_{\mathrm{R}}}\right)$. Consequently, we have $\Omega_0 = V\Delta_0^2/g + \sum_{\boldsymbol{k}} (\varepsilon_{\boldsymbol{k}} - \mu - E_{\boldsymbol{k}}) - \frac{2}{\beta} \sum_{\boldsymbol{k}} \ln\left(1 + \mathrm{e}^{-\beta E_{\boldsymbol{k}}}\right)$ with $E_{\boldsymbol{k}} = \sqrt{(\varepsilon_{\boldsymbol{k}} - \mu)^2 + \Delta_0^2}$.

In the presence of a quantized vortex considered in this paper, the saddle point ansatz can be chosen as $\Delta(\boldsymbol{r}, \tau) = \Delta_r \mathrm{e}^{\mathrm{i}\theta}$, where $r = \sqrt{x^2 + y^2}$ is the distance to the vortex line and θ the angle around the vortex in the cylindrical coordinates $\boldsymbol{r} = (r, \theta, z)$. With this ansatz, the effective action $S_{\mathrm{eff}} = \int_0^\beta \mathrm{d}\tau \int \mathrm{d}\boldsymbol{r} \Delta_r^2/g - \mathrm{Tr}\ln\left[\tilde{\boldsymbol{G}}^{-1}\right]$ has the same form as Eq. (4) with the inverse Green's function being

$$\tilde{\boldsymbol{G}}^{-1} = \begin{bmatrix} \partial_\tau + \hat{\xi}_{\boldsymbol{p}} - \dfrac{\mathrm{i}l}{2mr^2} \dfrac{\partial}{\partial\theta} + \dfrac{l^2}{8mr^2} & -\Delta_r \\ -\Delta_r & \partial_\tau - \hat{\xi}_{\boldsymbol{p}} + \dfrac{\mathrm{i}l}{2mr^2} \dfrac{\partial}{\partial\theta} - \dfrac{l^2}{8mr^2} \end{bmatrix}. \tag{9}$$

As have been pointed out in Ref. [43], $\frac{il}{2mr^2}\frac{\partial}{\partial\theta}$ is irrelevant to the low energy properties of the system and will be neglected in the following treatment. However, the partition function is still not integrable because of the inhomogeneous term $\frac{l^2}{8mr^2}$. Following Ref. [38] and [39], we assume that the paring field varies slowly in comparison with the relevant fermion frequencies and define a local chemical potential $\mu_r = \mu - 1/\left(8mr^2\right)$. Under this approximation and using the tight binding approximation for the band spectrum, we can obtain the thermodynamic potential

$$\begin{aligned}\Omega_{\rm v} &= V\frac{\Delta_r^2}{g} + \sum_{\boldsymbol{k}}\left(\varepsilon_{\boldsymbol{k}} - \mu_r - E_{\boldsymbol{k},r}\right)\\ &\quad - \frac{2}{\beta}\sum_{\boldsymbol{k}}\ln\left(1+\mathrm{e}^{-\beta E_{\boldsymbol{k},r}}\right),\end{aligned} \tag{10}$$

where $E_{\boldsymbol{k},r} = \sqrt{\left(\varepsilon_{\boldsymbol{k}} - \mu_r\right)^2 + \Delta_r^2}$. In this paper, we only consider the zero temperature case. Through variation of $\Omega_{\rm v}$ with respect to Δ_r, the gap equation can be obtained as

$$\frac{1}{g} = \frac{1}{V}\sum_{\boldsymbol{k}}\frac{1}{2E_{\boldsymbol{k},r}}, \tag{11}$$

and the density of the Fermionic atoms can be derived by $n_r = -\partial\Omega_{\rm v}/\partial\mu_r$,

$$n_r = \frac{1}{V}\sum_{\boldsymbol{k}}\left(1 - \frac{\varepsilon_{\boldsymbol{k}} - \mu_r}{E_{\boldsymbol{k},r}}\right). \tag{12}$$

Equations (11) and (12) are the generalized BCS mean-field equations in the presence of a single quantized vortex and an optical lattice potential. The bulk value of the chemical potential μ_0 and gap parameter Δ_0 have to be calculated by solving Eqs. (11) and (12) far away from the vortex core. From this, one can then obtain Δ_r and n_r for different parameters across the BCS–BEC and 3D–2D crossovers.

3. Vortex structure in the BCS–BEC crossover

As shown in Ref. [38], the atom density n_r and pair density Δ_r behave differently on BCS side and BEC side of the Feshbach resonance characterized by the formation of bound state in vacuum. Therefore, it is necessary to identify the resonance point in the presence of an optical lattice. This has been investigated intensively using the scattering theory.[44,45] In this paper, we use another simpler strategy[46] which reproduces qualitatively correct results but with much less numerical efforts. In the continuum limit, the momentum integration in the gap equation is ultra-violet divergent as a result of the use of the short range s-wave interaction, which implies a high momentum cut-off $k_\perp = \sqrt{k_x^2 + k_y^2} < k_0 \sim 1/R_0$ with R_0 being the effective interaction range. We now replace g in terms of the binding energy $\varepsilon_{\rm b} > 0$ through $1/g = 1/v\sum_{\boldsymbol{k}} 1/\left(2\varepsilon_{\boldsymbol{k}} + \varepsilon_{\rm b}\right)$, from which we obtain

$$\varepsilon_{\rm b} = \sqrt{\coth^2\left(\frac{1}{2G}\right)\left(\varepsilon_0^2 + 16t^2\sinh^2\left(\frac{1}{2G}\right)\right)} - \varepsilon_0 - 4t, \tag{13}$$

with $mg/4\pi d = G$ being the dimensionless interaction parameter and $\varepsilon_0 = k_0^2/2m$. The above equation reduces to Eq. (4) of Ref. [46] in the weak interaction limit. In the 2D limit $t = 0$, there is always a bound state for arbitrary interaction with the binding energy given by $\varepsilon_{\rm b} = \left[\coth\left(1/2G\right) - 1\right]\varepsilon_0$. But for finite t, there is a critical value $G_{\rm c}$ beyond which a bound state will form in the vacuum as shown in Fig. 1(a) with the red point denoting the critical value $G_{\rm c}$. Simple algebraic manipulation of Eq. (13) with $\varepsilon_{\rm b} = 0$ leads to

$$\frac{1}{G_{\rm c}} = 2\log\left(\sqrt{\varepsilon_0/4t} + \sqrt{\varepsilon_0/4t + 1}\right), \tag{14}$$

which is represented in Fig. 1(b).

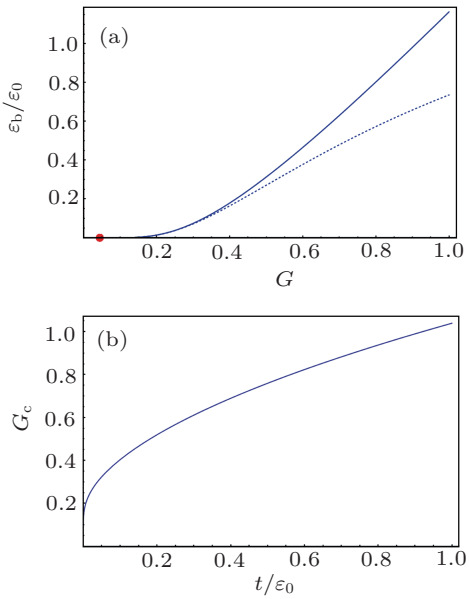


Fig. 1. (color online) (a) Binding energy as a function of the dimensionless interaction parameter G defined in the text. The solid line is the plot of Eq. (13) and dashed line is for the analytical results in the weakly interacting limit presented in Ref. [46]. The red dot denotes the critical interaction parameter beyond which a bound state will form. (b) Critical interaction parameter as a function of the lattice potential parameter t (Eq. (14)).

As shown in Ref. [38], the atoms can penetrate into the vortex core on the BCS side (no bound state) while not on the BEC (with bound state) side. With the critical value $G_{\rm c}$ obtained above, we can now investigate this peculiar feature for the system under consideration.

By self-consistently solving Eqs. (11) and (12) far away from the vortex $r \to \infty$, we can obtain Δ_0 and μ_0. The vertex profiles characterized by Δ_r and μ_r can then be obtained by solving Eqs. (11) and (12) and the numerical results are presented in Fig. 1. The interaction parameters used in the numerical calculations are chosen according to Eq. (14). Without loss of generality, the other parameters we used in the numerical evaluation are chosen as $k_{\rm F}d = 0.2$, $t = 0.5e_{\rm F}$, and $k_0 = 2\times10^4 k_{\rm F}$, with $k_{\rm F}$ being the Fermi momentum in the uniform space defined as $k_{\rm F}^3 = 3\pi^2 n$ and the corresponding Fermi energy $e_{\rm F} = k_{\rm F}^2/2m$. The numerical results are shown in Fig. 2.

It can be seen that on the BCS side with $G < G_c$, the atoms can penetrate into the vertex core while they cannot penetrate on the BEC side. Through detailed numerical investigations for various situations, we find that this picture happens for any optical lattice parameter t.

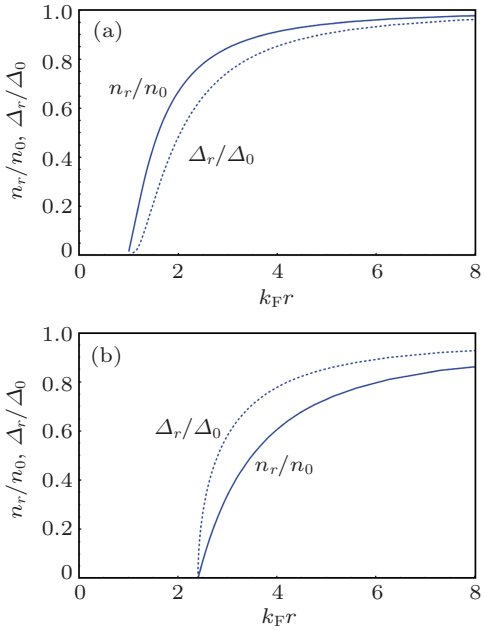


Fig. 2. (color online) Vortex profiles on (a) the BCS side with dimensionless interaction parameter $G = 0.045$ and (b) the BEC side with $G = 0.053$. The critical interaction parameter $G_c = 0.049$ is determined by Eq. (14) with other parameters being given as $k_F d = 0.2$, $t = 0.5 e_F$, and $k_0 = 2 \times 10^4 k_F$. Solid and dotted lines represent the atom number density and the pair density, respectively.

However, the present path-integral formalism used to describe the vortex state amounts to a local density approximation[38] and is invalid around the vortex core. The main reason for the breakdown is the assumption that the order parameter varies smoothly. Consequently, the vortex profiles shown in Fig. 2 are estimated to be wrong approaching the vortex core and one may resort to the BdG equation which is more accurate in the vortex core region. Despite this defect, the theory naturally gives another important quantity r_v, the vortex core size, which will be discussed in detail in the following section.

4. Vortex size

The vortex core size r_v can be defined as the distance from the vortex core at which the order parameter becomes zero, as shown in Fig. 2. Numerical solutions of r_v as a function of dimensionless interaction parameter G are represented in Fig. 3, with other parameters chosen the same as those used to obtain Fig. 2. One can see that, in the BCS limit, the vortex core size approaches a constant value, which agrees with the results in Ref. [38]. However, in the BEC limit, the vortex core size tends to a constant instead of growing with increasing interaction strength in the homogeneous space shown in Ref. [38].

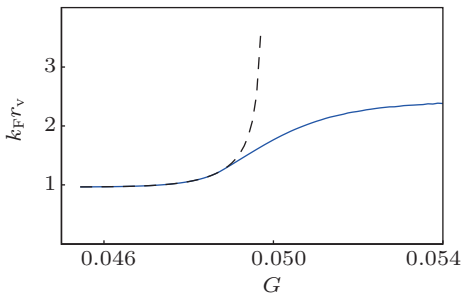


Fig. 3. (color online) Vortex core size as a function of the dimensionless interaction parameter G. The lattice parameters are chosen to be the same as those used to obtain Fig. 2. The solid blue line represents the numerical results obtained from the self-consistent solutions of Eqs. (11) and (12). The dashed black line is the asymptotic behavior (Eq. (15)) of the vortex core size in the BCS regime.

In order to understand the asymptotic behaviors of the vortex core size in the BCS and the BEC limits, we analyze the properties of the gap equation (Eq. (11)) and number equation (Eq. (12)) approaching the vortex core. By setting $\triangle_r = 0$, one can easily check that the momentum integration on the right side of Eq. (11) is divergent for $\mu_r > 0$. Therefore, the only acceptable solution for the local chemical potential at the vortex core should be $\mu_r \leq 0$. Besides, the atom density in the vortex core also goes to zero for $\mu_r \leq 0$. In conclusion, the local chemical potential should satisfy $\mu_r \leq 0$ approaching the vortex core.

In the BCS regime, the bulk chemical potential $\mu_0 > 0$. Since the momentum integral is divergent for positive local chemical potential, the gap equation can be satisfied for any $\mu_r > 0$ with $\Delta_r \to 0$. Therefore, the vortex core size should be determined by the number equation with the critical condition being $n_r = 0$, which leads to $\mu_r = 0$. Finally, we obtain

$$r_v = \sqrt{\frac{1}{4m\mu_0}}, \tag{15}$$

which is plotted as the dashed line in Fig. 3. In the deep BCS limit, $\mu_0 \to E_F$ and $r_v \to 1/(2k_F)$, which agrees with the result obtained in Ref. [38]. Note that in Fig. 3, $k_F r_v$ does not go to $1/2$ because k_F is the Fermi momentum in the homogeneous space. If we used the proper Fermi momentum and energy in the presence of the optical lattice, we would obtain the same numerical results as those shown in Ref. [38].

In the BEC limit, since the bulk chemical potential $\mu_0 \sim -\varepsilon_b/2$ and hence $\mu_r < 0$, $n_r = 0$ is always satisfied for arbitrary r at the vortex core. Therefore, the vortex core size should be determined by the gap equation. Since $\mu_r < 0$, the momentum integral is convergent and the vortex core size can be obtained analytically from the following equation:

$$G = 2\log\frac{\sqrt{\varepsilon_0+\mu_r}+\sqrt{\varepsilon_0+\mu_r+4t}}{\sqrt{\mu_r}+\sqrt{\mu_r+4t}}. \tag{16}$$

As can be seen in Fig. 3, r_v tends to be a constant instead of growing with increasing interaction strength in the case without the optical lattice trap. As stated in Ref. [38], in the BEC limit, the vortex core size is identified as the

healing length $1/\sqrt{4\pi n a_{\rm m}}$ since the system can be considered as a Bose–Einstein condensate of tightly bound molecules with weak repulsive interactions. On the mean-field level, the molecular scattering length $a_{\rm m} = 2a_0$ with a_0 being the scattering length of Fermi atoms with opposite spins. However, in the presence of the optical lattice potential, the interaction between molecules is a constant.[46] Consequently, the vortex core size saturates to a fixed value approaching the BEC limit, as depicted in Fig. 3.

5. Conclusion and outlooks

In summary, we have extended the path-integral mean-field theory for the vortex state to the case with an optical lattice trapping potential. In the low energy limit, we only considered the lowest band and used a Hubbard-type spectrum to effectively describe the effects of the periodic potential. Within the path-integral formalism, we derived the mean-field number and gap equation which were then solved self-consistently to obtain the vortex profiles and the vortex core size. For the vortex profile characterized by the atom number density and pair density, like the homogeneous case, we found that the atoms can penetrate into the vortex core in the BCS regime while it cannot occur in the BEC regime. The dimensional effect was also discussed by calculating the bound state energy as a function of the interaction and lattice parameters. We found that the bound state emerges only when the interaction strength is bigger than a critical value. From the vortex profiles, we also obtained the vortex core size as a function of the interaction parameter. By analyzing the atom number and gap equations at the vortex core, we found that the vortex core size is determined by the atom number equation in the BCS regime for positive bulk chemical potential and by the gap equation in the BEC regime for negative bulk chemical potential.

The mean-field approximation is problematic near the vortex core. Therefore, it is important to know how the vortex profile evolves in the dimensional crossover by using a beyond mean-field theory, like the BdG equation[37] and the beyond-mean-field corrections.[47,48] Besides, the vortex properties in the presence of other trapping potentials and spin–orbit coupling are also under investigations.

References

[1] Anderson M H, Ensher J R, Matthews M R, Wieman C E and Cornell E A 1995 *Science* **269** 198
[2] DeMarco B and Jin D S 1999 *Science* **285** 1703
[3] Truscott A, Strecker K, McAlexander W, Partridge G and Hulet R G 2001 *Science* **291** 2570
[4] O'Hara K M, Hemmer S L, Gehm M E, Granade S R and Thomas J E 2002 *Science* **298** 2179
[5] Bourdel T, Cubizolles J, Khaykovich L, Magalhaes K, Kokkelmans S, Shlyapnikov G and Salomon C 2003 *Phys. Rev. Lett.* **91** 020402
[6] Bartenstein M, Altmeyer A, Riedl S, Jochim S, Chin C, Hecker-Denschlag J and Grimm R 2004 *Phys. Rev. Lett.* **92** 120401
[7] Bourdel T, Khaykovich L, Cubizolles J, Zhang J, Chevy F, Teichmann M, Tarruell L, Kokkelmans S J J M F and Salomon C 2004 *Phys. Rev. Lett.* **93** 050401
[8] Regal C A, Greiner M and Jin D S 2004 *Phys. Rev. Lett.* **92** 040403
[9] Zwierlein M W, Stan C A, Schunck C H, Raupach S M F, Kerman A J and Ketterle W 2004 *Phys. Rev. Lett.* **92** 120403
[10] Giorgini S, Pitaevskii L P and Stringari S 2008 *Rev. Mod. Phys.* **80** 1215
[11] Bloch I, Dalibard J and Zwerger W 2008 *Rev. Mod. Phys.* **80** 885
[12] Deng J, Diao P P, Yu Q L and Wu H B 2015 *Chin. Phys. Lett.* **32** 53401
[13] Chen K J and Zhang W 2014 *Chin. Phys. Lett.* **31** 110303
[14] Luan T, Jia T, Chen X Z and Ma Z Y 2014 *Chhin. Phys. Lett.* **31** 43401
[15] Qi X Y, Zhang A X and Xue J K 2013 *Chin. Phys. Lett.* **30** 110305
[16] Ruan X X, Gong H, Du L, Jiang Y, Sun W M and Zong H S 2013 *Chin. Phys. Lett.* **30** 110303
[17] Liu Y X, Ye J, Li Y Y and Zhang Y B 2015 *Chin. Phys. B* **24** 86701
[18] Feshbach H 1958 *Ann. Phys.* **5** 357
[19] Stoof H T C, Houbiers M, Sackett C A and Hulet R G 1996 *Phys. Rev. Lett.* **76** 10
[20] Bardeen J, Cooper L N and Schrieffer J R 1957 *Phys. Rev.* **108** 1175
[21] Eagles B 1969 *Phys. Rev.* **186** 456
[22] Leggett A J 1980 *J. Phys. Colloq.* **41** 7
[23] Zwierlein M W, Abo-Shaeer J R, Schirotzek A, Schunck C H and Ketterle W 2005 *Nature* **435** 1047
[24] Li S Q, Hu H and Liu X J 2008 *Physics* **37** 141
[25] Zhang J and Zhai H 2006 *Physics* **35** 553
[26] Lai X J, Cai X O and Zhang J F 2015 *Chin. Phys. B* **24** 70503
[27] Wen H H 2006 *Physics* **35** 16
[28] Wen H H 2006 *Physics* **35** 111
[29] Lü G, Cao X C, Qin Y F, Wang L H, Li G H, Gao F, Sun F W and Zhang H 2015 *Acta Phys. Sin.* **64** 217501 (in Chinese)
[30] Sun L, Huo Y, Zhou C, Liang J H, Zhang X Z, Xu Z J, Wang Y and Wu Y Z 2015 *Acta Phys. Sin.* **64** 197502 (in Chinese)
[31] Liu X L, Yang Y, Wu J P, Zhang Y F, Fan H M and Ding J 2015 *Chin. Phys. B* **24** 127505
[32] Sun M J and Liu Y W 2015 *Acta Phys. Sin.* **64** 247505 (in Chinese)
[33] Bulgac A and Yu Y 2003 *Phys. Rev. Lett.* **91** 190404
[34] Hu H, Liu X J and Drummond P 2007 *Phys. Rev. Lett* **98** 060406
[35] Sensarma R, Randeria M and Ho T L 2006 *Phys. Rev. Lett.* **96** 090403
[36] Machida M and Koyama T 2005 *Phys. Rev. Lett.* **94** 140401
[37] de Gennes P G 1966 *Superconductivity of Metals and Alloys* (New York: Benjamin)
[38] Tempere J, Wouters M and Devreese J T 2005 *Phys. Rev. A* **71** 033631
[39] Tempere J and Devreese J T 2006 *Physica C* **437–438** 323
[40] Tempere J and Devreese J T 2005 *Path-integrals and the BEC/BCS Crossover in Dilute Atomic Gases. The 8-th International Conference "Path Integrals. From Quantum Information to Cosmology"*, Prague, Czech Republic
[41] Altland A and Simons B D 2010 *Condensed Matter Field Theory* (Cambridge: Cambridge University Press)
[42] Bhattacherjee A B 2007 *J. Phys. B: At. Mol. Opt. Phys.* **40** 4453
[43] De Palo S, Castellani C, Di Castro C and Chakraverty B K 1999 *Phys. Rev. B* **60** 564
[44] Orso G, Menotti C and Stringari S 2006 *Phys. Rev. Lett.* **97** 190408
[45] Wouters M and Orso G 2006 *Phys. Rev. A* **73** 012707
[46] Iskin M and Sá de Melo C A R 2009 *Phys. Rev. Lett.* **103** 165301
[47] Adhikari S K andSalasnich L 2008 *Phys. Rev. A* **78** 043616
[48] Adhikari S K 2010 *J. Phys. B* **43** 085304